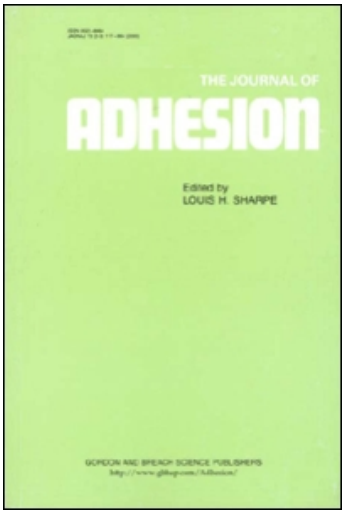

The Journal of Adhesion

Publication details, including instructions for authors and subscription information:
http://www.informaworld.com/smpp/title~content=t713453635

Mixed-Mode Cathodic Delamination of Rubber From Steel

K. M. Liechti[a]; W. Adamjee[ab]
[a] Department of Aerospace Engineering and Engineering Mechanics, The University of Texas at Austin, Austin, Texas, USA [b] Motorola, Inc., Austin, TX, USA

To cite this Article Liechti, K. M. and Adamjee, W.(1992) 'Mixed-Mode Cathodic Delamination of Rubber From Steel', The Journal of Adhesion, 40: 1, 27 — 45
To link to this Article: DOI: 10.1080/00218469208030469
URL: http://dx.doi.org/10.1080/00218469208030469

J. Adhesion, 1992, Vol. 40, pp. 27–45
Reprints available directly from the publisher
Photocopying permitted by license only

Printed in the United States of America.

Mixed-Mode Cathodic Delamination of Rubber From Steel*

K. M. LIECHTI and W. ADAMJEE**

Department of Aerospace Engineering and Engineering Mechanics, The University of Texas at Austin, Austin, Texas 78712, USA

(Received April 27, 1992; in final form July 27, 1992)

A series of scarf specimens with a range of scarf angles was used to examine the effect of fracture mode-mix on the cathodic delamination of rubber from steel in an aggressive (1N NaOH) environment. Fracture parameters were extracted from finite element analyses that accounted for the nonlinearly elastic response and the finite deformations in the rubber layer. Delamination growth rates were found to be independent of energy release rate levels that were chosen for the study but were strongly dependent on crack opening angle, the parameter that was used to represent the local fracture mode-mix.

KEY WORDS debonding; rubber; steel; mixed-mode fracture; cathodic delamination; environmentally assisted crack growth.

INTRODUCTION

Rubber-to-metal bonds are used in a number of primary structural components in automotive, naval, offshore oil production and civil engineering applications. Although satisfactory bonds have been routinely obtained, even in marine environments,[1] the presence of a cathodic potential can rapidly degrade rubber-to-metal joints. The electrochemical mechanisms that give rise to cathodic delamination have been examined in a number of publications.[2-4] Cathodic delamination gives rise to sub-critical crack growth which is the hallmark of any environmentally-assisted crack propagation. As a result, the resistance to cathodic delamination may be characterized in a phenomenological manner by correlating crack growth rates with a suitable fracture parameter.[5] However, interfacial crack growth is inherently mixed-mode in nature because the direction of crack growth is the same irrespective of the ratio of globally applied tensile and shear loads. This complicates the choice of fracture parameter, especially when a wide range of fracture mode-mixes has to be considered.

*Presented at the 14th Annual Meeting of The Adhesion Society, Inc., Clearwater, Florida, U.S.A., February 17–20, 1991.

**Current address: Motorola, Inc., Austin, TX, USA.

The potential influence of mode-mix effects has been dramatically suggested by observations that cathodic delamination did not occur under pure shear loadings.[1,6] Additionally, in some work that made use of strip blister specimens with a range of rubber thicknesses, it was noted[7] that crack growth rates varied with rubber layer thickness even though load levels ensured that similar energy release rates were in effect. Although variations in mode-mix due to crack length and layer thickness were not extracted, the fracture mode-mix is expected to vary with both parameters, even under large deflections.[8] It is possible that the noted variations in crack growth rates with rubber layer thickness were due to the concommittant variations in fracture mode-mix. This possibility, and the observations of zero delamination under shear, motivated the present study where the effect of fracture mode-mix on cathodic delamination growth rates has been examined in a quantitative manner.

There were essentially three aspects to the study: first it was necessary to obtain a realistic model of the nonlinearly elastic response of the Neoprene 5109S that was used in the cathodic delamination experiments; the second phase dealt with the extraction of fracture parameters; the final step was to conduct cathodic delamination experiments using a series of scarf specimens and make correlations between crack growth rates and energy release rates and crack opening angle, which was taken as a measure of the fracture mode-mix. The first two aspects are described in the stress analysis section of the paper and the third is covered under cathodic delamination.

STRESS ANALYSIS

The modeling and experimental procedures that were used to obtain the nonlinearly elastic response of the Neoprene 5109S have been described in detail elsewhere.[5,9] A number of models were considered but the most satisfactory ones were those due to Peng[10] and Ogden.[11] Both models depart from previous approaches in that their strain energy density functions, W, are expressed in terms of the principal stretches, λ_i, rather than the stretch invariants. Although both models can accommodate compressibility, the Neoprene 5109S was found to be essentially incompressible, thus allowing simpler representations to be made. Uniaxial tension and strip biaxial tests were conducted in order to extract the parameters required for each model.

In the representation due to Peng,[10] the derivative of the strain energy density function, $W'(\lambda_i)$, is obtained from discretizations of the uniaxial and strip biaxial responses. The resulting curve for the Neoprene 5109S is shown in Figure 1 and was input directly into the finite element code TEXPAC-NL[12] which was used in the stress analysis. In essence, once $W'(\lambda_i)$ has been determined, the true stresses, t_i, in the principal directions ($i=1,2,3$) are given by

$$t_i = \lambda_i W'(\lambda_i) + p \tag{1}$$

where p is the hydrostatic pressure which must be included because of the incompressibility constraint. Included in this approach is the concept of separability, first introduced by Valanis and Landel,[13] where the strain energy density function

$$W = W(\lambda_1) + W(\lambda_2) + W(\lambda_3) \tag{2}$$

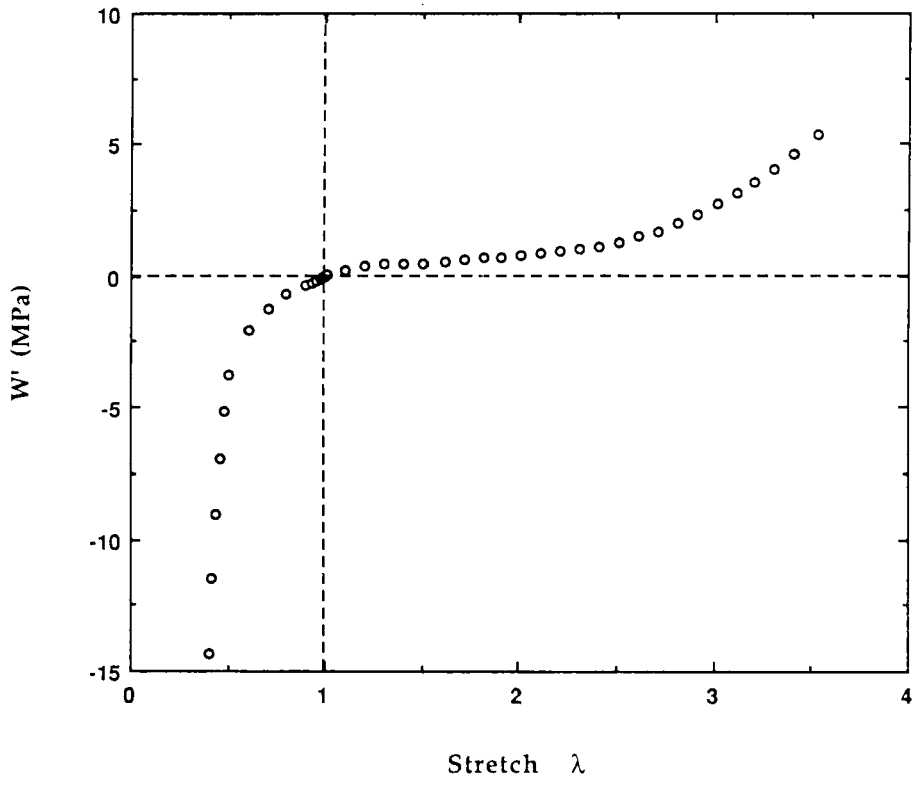

FIGURE 1 Derivative of the Strain Energy Density Function for Neoprene 5109S (Peng Model).

The representation due to Ogden[11] has an analytical form where

$$W = \sum_{r=1}^{N} \eta_r \psi(\alpha_r) \tag{3}$$

and

$$\psi(\alpha_r) = (\lambda_1^{\alpha_r} + \lambda_2^{\alpha_r} + \lambda_3^{\alpha_r})/\alpha_r \tag{4}$$

The true stress can then be written as

$$t_i = \sum_{r=1}^{N} \eta_r \lambda_i^{\alpha_r} + p \tag{5}$$

The parameters η_r and α_r were calculated on the basis of the uniaxial and strip biaxial tests. A three-term summation with the parameters as indicated in Table I fit the uniaxial and strip response of Neoprene 5109S.

Both models and the finite element code were checked for internal consistency by simulating the uniaxial and strip biaxial tests. The question as to which model was more applicable to the response of the scarf specimens intended for use in the

TABLE I
Parameters for the Ogden model

r	η	α
1	1.40 MPa	1.3
2	2.07 kPa	7.0
3	−20.68 kPa	−5.0

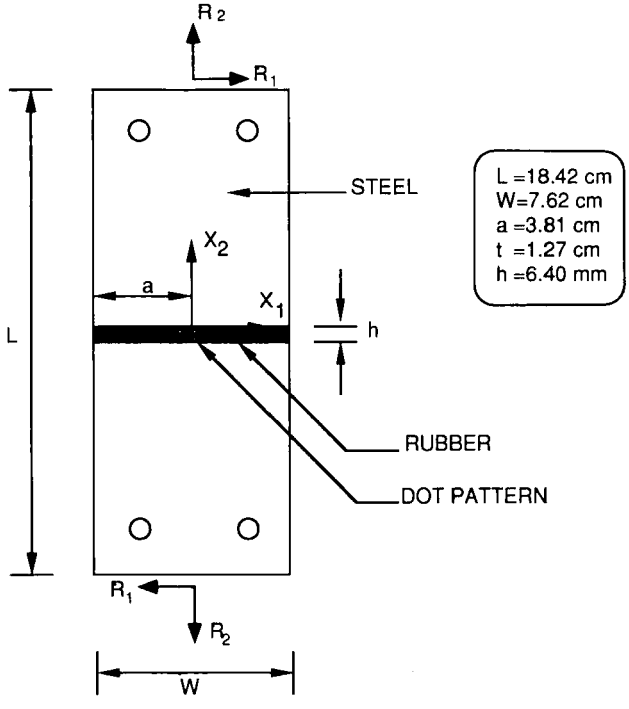

a) Validation Specimen

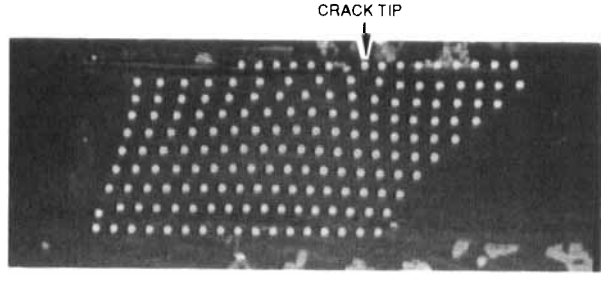

b) Deformed Dot Pattern

FIGURE 2 Validation Specimen for Rubber Elasticity Models.

delamination experiments was resolved by examining the response of a validation specimen (Fig. 2a) whose rubber layer thickness and height matched those of the scarf specimens.

The rubber layer was 6.35 mm high, 12.7 mm thick, and 76.2 mm long, with a nominally 38.1 mm initial crack (delaminated region). The specimen was prepared by molding, with the rubber bonded to the steel using the Chemlock 205/220 primer/adhesive system (Lord Corp., Erie, PA, USA). The initial delamination was made by masking the steel with Teflon® tape prior to the application of the adhesive. After the molding, flashing was removed by carefully sanding the specimen surface and cleaning it with alcohol to provide a clean boundary at the rubber steel interfaces. To serve as a measure of the displacement field, white dots, made by Chartpak Transfer Lettering Co.,† with a density of 1.69 dots/mm^2 were transferred on the surface over a square region surrounding the crack tip. A light coat of water-based glue was applied to the rubber surface to improve the adhesion of the dots.

The specimen was loaded in simple shear using a biaxial loading device[14] at a rate of 0.025 mm/sec. The reactions normal and tangential to the bondline were measured using load cells that were attached to the grips. The movement of the dots was tracked with a video camera and recorded with elapsed time on a high resolution video cassette recorder. The recordings were subsequently analyzed using a digital image analysis system where the centroidal coordinates of the dots in the deformed configuration were subtracted from those in the undeformed configuration to yield u_1 and u_2, the displacements parallel and normal to the bondline.

The displacements were measured along a number of profiles $x_2 =$ constant, where x_2 was the distance from the cracked interface. The results for the profile closest to the interface ($x_2/h = 0.08$) can be found in Figure 3 where the displacement components are normalized by the applied displacement u_0. The measured displacements are compared with those obtained from three-dimensional analyses that incorporated the representations due to Peng and Ogden. The mesh for the three-dimensional analyses was constructed by layering a two-dimensional mesh through the thickness. The elements used were 20-node isoparametric brick elements with quadratic displacements. The steel was considered to be rigid with respect to the rubber and, since the primer and adhesive layers were very thin (7.6 and 25.4 μm, respectively) and two orders of magnitude stiffer than the rubber, their presence was neglected. The nodal displacements from the finite element solutions were interpolated using the element shape functions so that they could be compared at the original locations of the transfer dots.

It can be seen from Figure 3 that the u_1 displacements obtained from the finite element solution that made use of the Ogden model slightly overpredicted but were consistently closer to the measured values. Displacements obtained from the Peng model also overpredicted u_1 values but the error was greater, more than 10 times measurement error ($u_i/u_0 = 0.01$). The picture for the u_2 displacements was less conclusive, mainly due to the fact that their values were almost within the error

†Thanks are due to Dr. J. A. Donavan, Department of Mechanical Engineering, University of Massachusetts at Amherst for sharing a special order of Chartpak sheets with us.

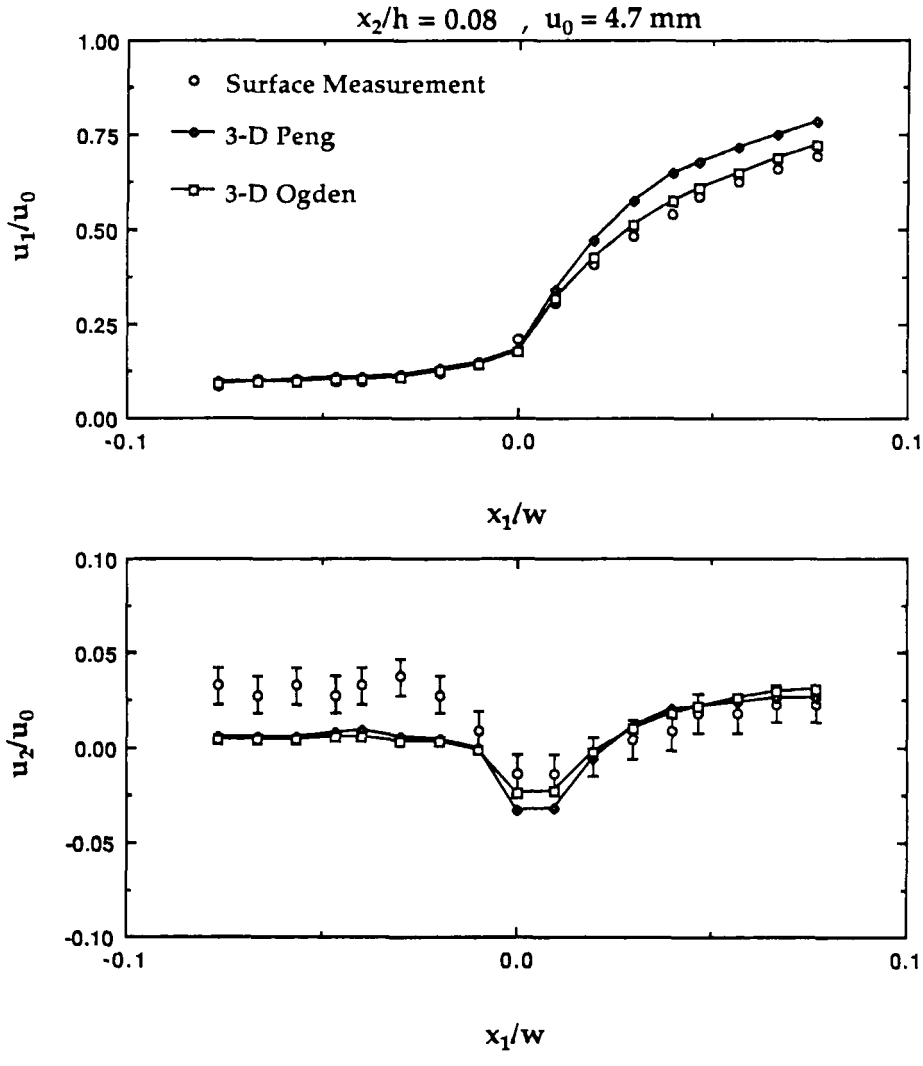

FIGURE 3 Comparison of Measured and Predicted In-plane Displacements in the Validation Specimen.

levels of the measurements. However, over the crack front, the values of u_2 obtained using the Ogden model were closer to the measured values.

A second basis for comparison of the performance of the models was the load reactions (Fig. 4) parallel (R_1) and perpendicular (R_2) to the bondline. The measured values of R_1 and R_2 were obtained from load cells. The predictions were obtained by summing the nodal point reactions along the displaced boundaries. The solutions for the R_1 component were both in very good agreement with the measured values for all levels of applied shear strain. The R_2 values predicted by the Peng model exhibited a strong compressive divergence for global strains greater than 30%. The measurements and the predictions for the Ogden model exhibited

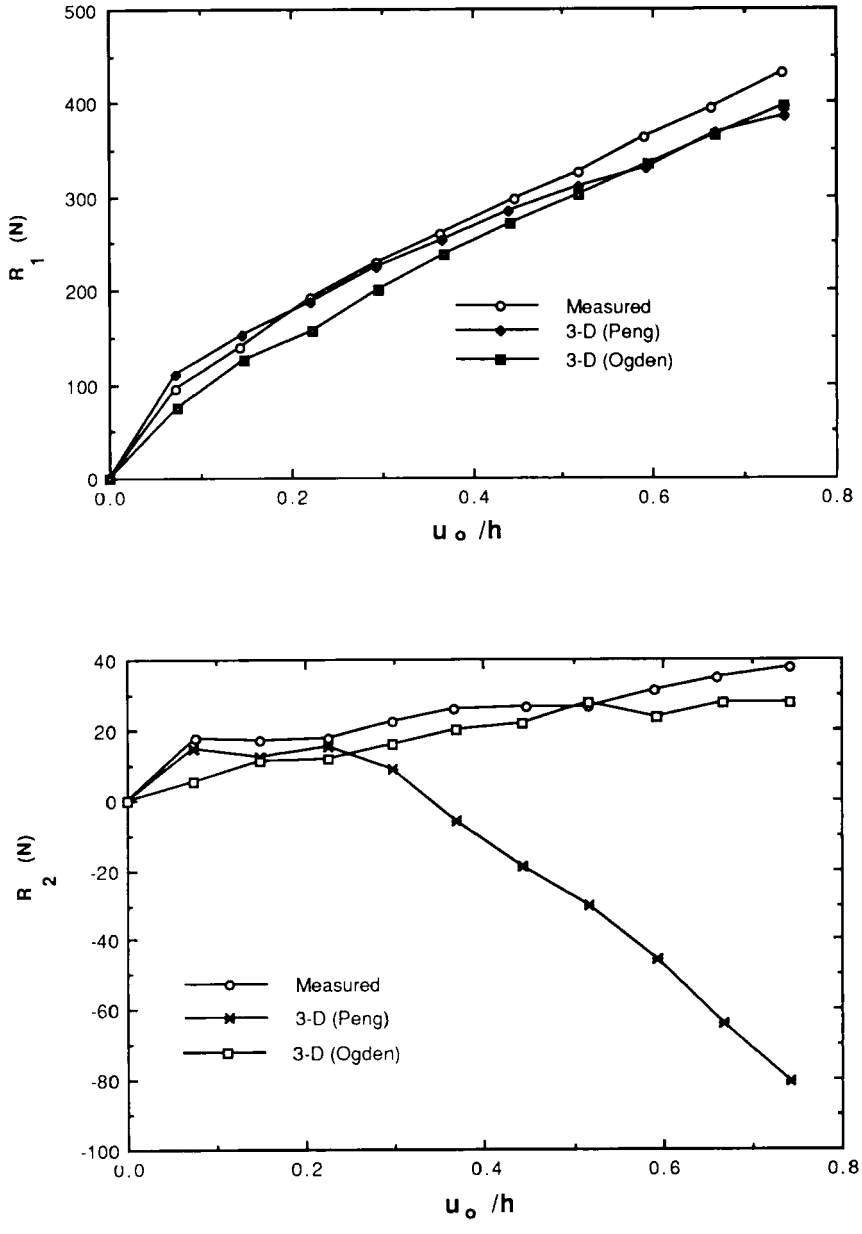

FIGURE 4 Comparison of Measured and Predicted Reactions in the Validation Specimen.

very little normal stress effect over the range of applied shear strains that was examined. In light of the comparisons made in Figure 3 and 4, the model due to Ogden was taken to be most representative of the response of Neoprene 5109S in the scarf specimens to be used in the cathodic delamination experiments.

The three-dimensional version of TEXPAC-NL did not provide any facility for

energy release rate calculations, other than calculating the change in energy release from two solutions where the crack length differs by a small amount. This approach was considered to be too time consuming and cumbersome, particularly in view of the fact that the two-dimensional version calculates the energy release rate through a virtual crack extension technique.[5] Having chosen the Ogden representation, the measurements that were made on the validation specimen were then used to determine whether plane-strain or plane-stress analyses of the scarf specimens would be more valid.

The first step (Fig. 5) was to compare the in-plane displacements obtained from

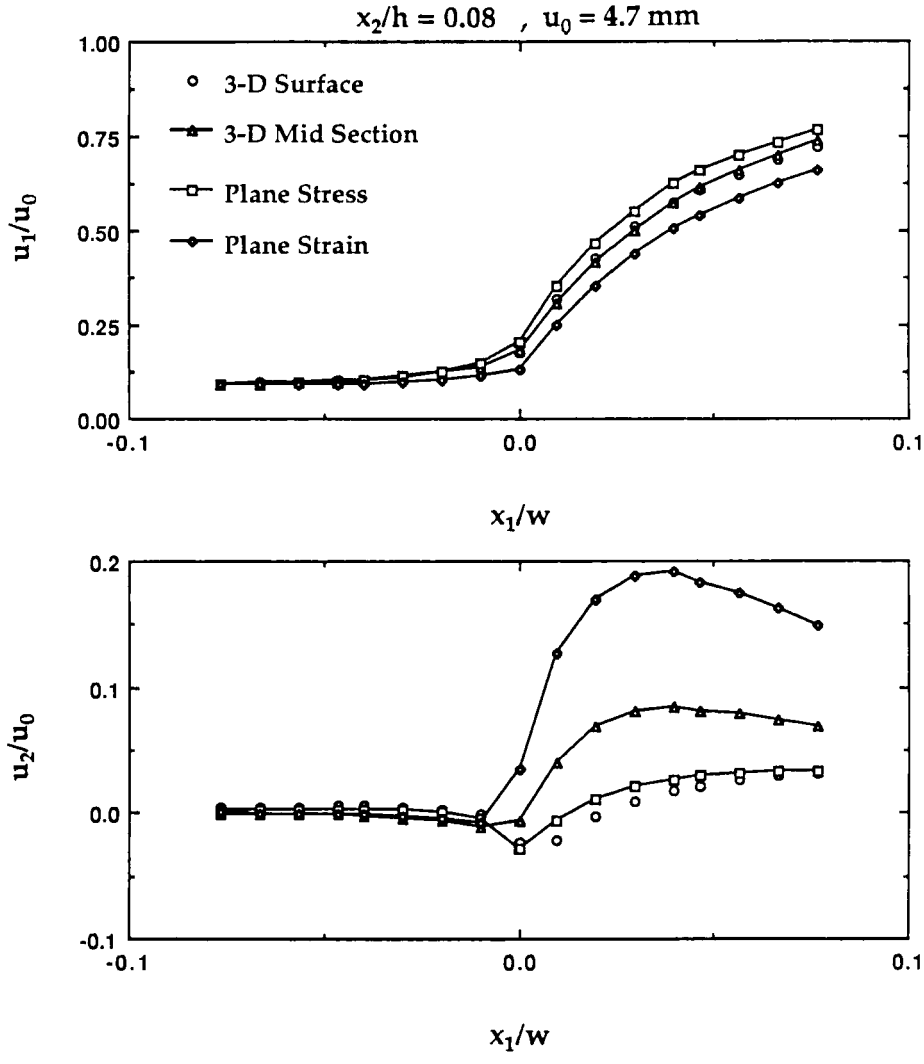

FIGURE 5 Comparison of In-plane Displacements Obtained from Measurements, Plane and Three-Dimensional Analyses (Ogden Model).

the surface and interior using a three-dimensional analysis with those obtained from plane-strain and plane-stress analyses. For the u_1 displacement component there was very little difference between the surface and interior solutions obtained from the full three-dimensional analysis. As a result, it was somewhat surprising to find that the plane-stress solution over predicted displacements and the plane-strain solution under predicted displacements to a greater extent. For the bond-normal displacements, u_2, the three-dimensional surface displacements were in best agreement with the plane-stress solution. Behind the crack, the displacements in the interior and those derived from the plane-strain solution were both larger than the surface displacements but were not in agreement themselves. These results suggested that plane-stress solutions of the scarf specimens would be valid, a conclusion that was strengthened by examining the load reactions obtained from the various solutions.

Both reactions obtained from plane-strain solutions were considerably larger than those corresponding to any other solution (Fig. 6). On the other hand, the plane-stress reactions in both directions were in very good agreement with the values obtained from the three-dimensional analysis. Another interesting difference[9] in the plane-stress and strain solutions was that the former indicated that energy release rates were independent of crack length for crack lengths in the range $0.25 \leq a/W \leq 0.75$. When plane-strain solutions were examined, there was an increase in energy release rates associated with increasing crack length. As will be seen later, cathodic delamination rates were also constant, lending further justification to the use of plane-stress analyses for extracting fracture parameters for the scarf specimens.

CATHODIC DELAMINATION

The main objective of the cathodic delamination experiments conducted here was to examine the effect of fracture mode-mix on delamination growth rates. Previous work[5,7] had indicated that crack growth rates were affected by the energy release rate levels in certain ranges. There appeared to be a threshold value in energy release rates below which there was no delamination. Immediately above this threshold, delamination of growth rates increased sharply, possibly because, at these rates, diffusion affected the delamination process and diffusion itself would be accelerated by higher energy release rates. The sharp increase in delamination rates was followed by a "plateau" region where delamination rates were relatively independent of energy release rate levels. In this regime it is likely that delamination rates are of the same order as diffusion rates so that delamination is no longer controlled by diffusion effects. Although not delineated by any results obtained to date, one expects that as energy release rate levels start to approach the adhesive fracture toughness of the bond ($\sim$10 kJ/m^2),[15] delamination growth rates would again increase with increasing energy release rate levels.

The effect of fracture mode-mix was examined in the plateau region where any inadvertent variations in energy release rate levels would not obscure the results. Examining mode-mix effects in the diffusion-controlled region would be very diffi-

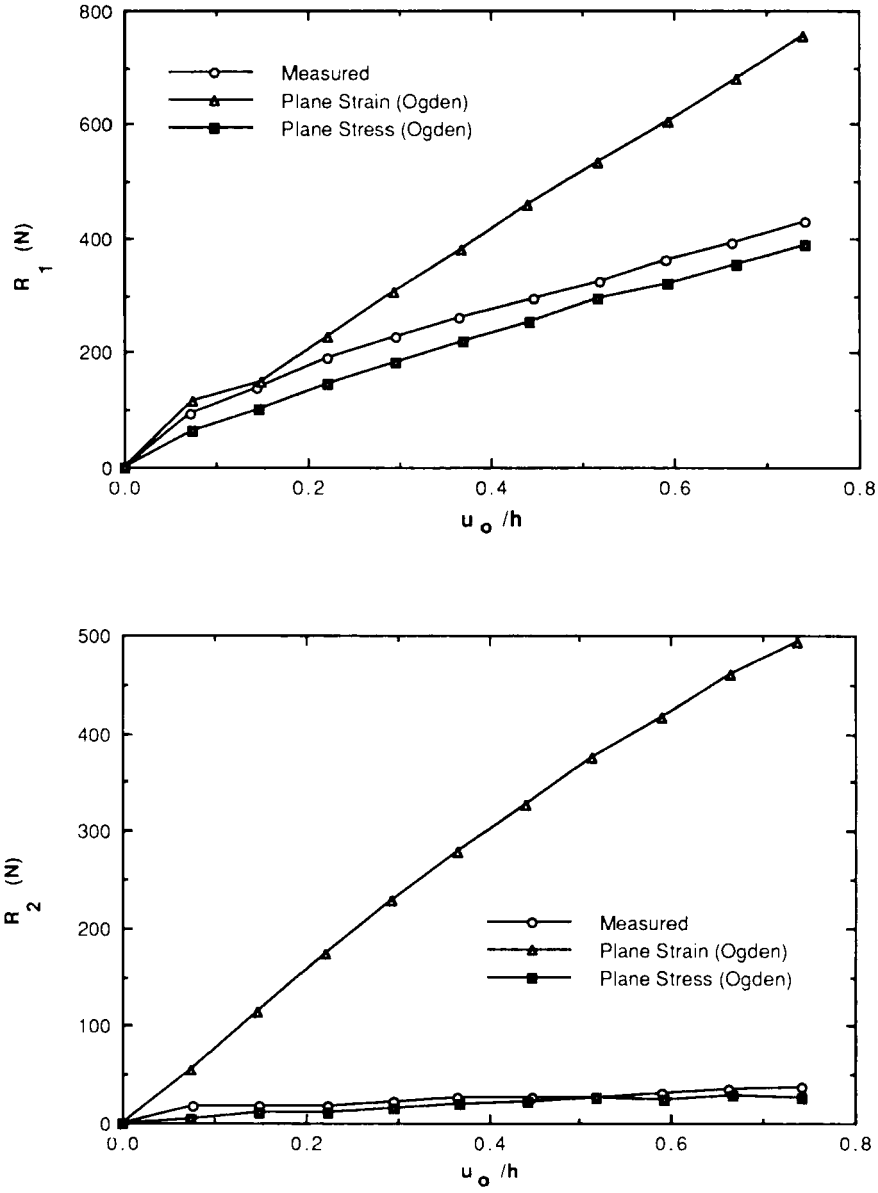

FIGURE 6 Reactions from Plane and Three-Dimensional Analyses of the Validation Specimen (Ogden Model).

cult due to the strong dependence of delamination growth rates on energy release rate levels there. The scarf specimen shown in Figure 7 was used to apply a range of fracture mode-mixes by changing the scarf angle, β.

The specimens consisted of steel adherends and a layer of Neoprene 5109S joined by the same Chemlok 205/220 primer and adhesive combination that had been used in previous work[5,7] and the validation specimen. In all specimens the rubber layer

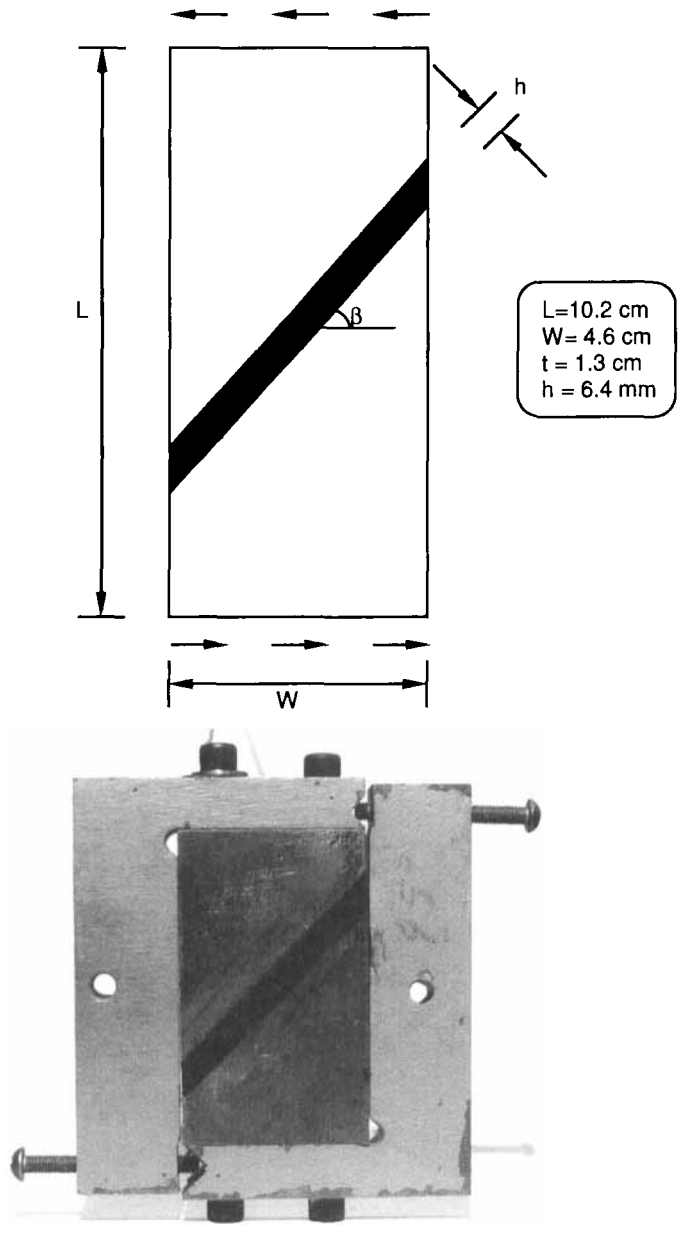

FIGURE 7 Scarf Specimen for the Cathodic Delamination Experiments.

height, thickness and the nominal initial debond length were 6.4 mm, 12.7 mm and 12.7 mm, respectively. Scarf angles of 0°, 10°, 30°, and 45° were used for the cathodic delamination experiments. The steel adherends were connected to a compact, two-piece loading frame (Fig. 7b) which applied a simple shear to the specimen through a pair of set screws.

Although the scarf angle, β, gives some indication of the fracture mode-mix, it is a global measure which may not completely reflect local effects, particularly in view of the finite deformations and nonlinearly elastic response of the rubber layer. In addition, since the usual separations of mode I and II stress intensity factors or energy release rates can no longer be made, the crack opening angle (COA), ϕ, was used as a local measure of fracture mode-mix. The relative COA as defined here relates to the proportion of bond-normal to bond-tangential crack opening displacements, Δu_2 and Δu_1, respectively. That is

$$\tan \phi = \frac{\Delta u_2}{\Delta u_1} \tag{6}$$

where $\Delta u_i = u_i^+ - u_i^-$, the difference between the displacement components of the upper and lower crack faces. According to this definition, a larger COA implies a larger mode I component.

One potential problem with fracture parameters that are based on crack opening displacements is the degree of arbitrariness that enters in specifying just how far behind the crack front the crack opening displacements are to be evaluated. However, when the nodal displacements from the finite element solution were interpolated it was found (Fig. 8) that ϕ was independent of the distance, r, from the crack front for $r < 0.5\mu m$. The variation in ϕ that is shown in Figure 8 was for a

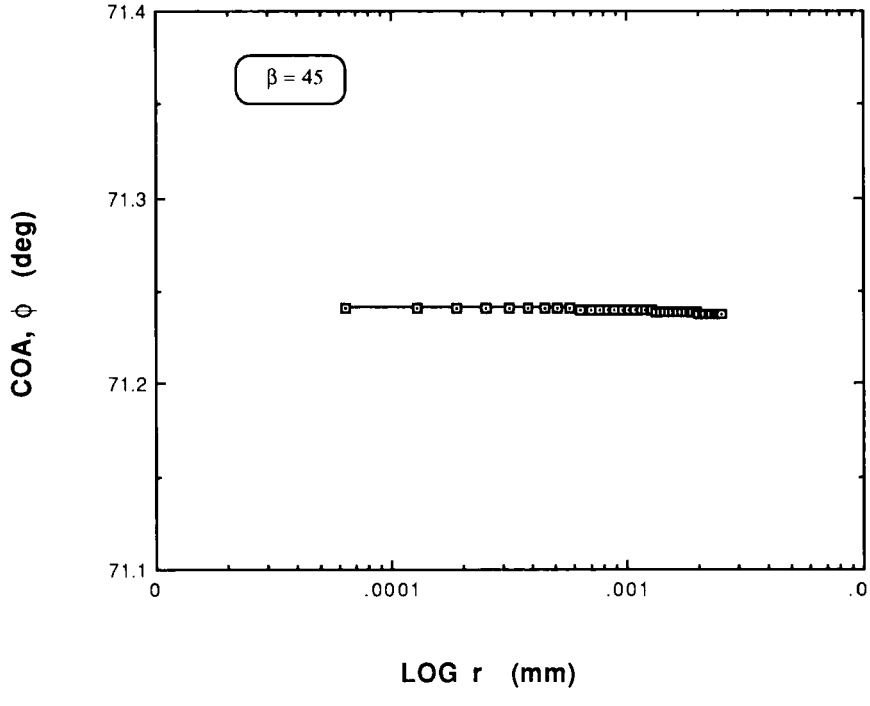

FIGURE 8 Variation of Crack Opening Angle with Distance from the Crack Front.

scarf angle of 45° and was the most severe; the region over which ϕ was constant was greater for the smaller scarf angles. It is not clear at this time how general this result is. The question was not addressed in the asymptotic analysis of Knowles and Sternberg[16] or the detailed finite element analyses of Ravichandran and Knauss.[17] In view of the observation presented here and its practical usefulness, the question certainly warrants further study. In any case, crack opening angles quoted in this paper were extracted at $r = 0.5\mu m$.

A series of plane-stress analyses of the scarf specimens were conducted for scarf angles of 0, 10, 30 and 45° and crack lengths in the range $0.50 \leq a/W \leq 0.85$. The variation in energy release rate, G, and crack opening angle, ϕ, with load level is shown in Figure 9. Both G and ϕ were independent of the crack lengths that were analyzed here.[9] The crack opening angle had a slight dependence on load level and did not have a one-to-one relationship with scarf angle. First, there was a small nonzero value of ϕ associated with zero scarf angle. This is a consequence of the nonlinearities in the problem in the sense that a linearly elastic, small strain analysis of an interfacially cracked body made up of an incompressible material on a rigid substrate predicts no coupling between mode I and mode II. Secondly, there was a strong increase in ϕ with β, roughly $\phi = 2\beta$ for $\beta < 30$ with a levelling off thereafter. The choice of scarf angles for the cathodic delaminations experiments thus provided a range of crack opening angles from $4° \leq \phi \leq 72°$.

The conditions for accelerated cathodic delamination were provided by placing the specimen in a 1N aqueous NaOH solution and applying a suitable electrical potential to the specimen (Fig. 10). The solution was maintained at a constant temperature of 30°C and was aerated to bring oxygen to the environment. A constant supply of oxygen was necessary because the dominant reaction in the delamination process involved a reduction of oxygen. The air was passed through a CO_2 trap to eliminate the formation of Calcium Carbonate encrustations in the tank. A potentiostat was used to maintain the steel parts of the specimen at a constant potential of -0.9 volts with respect to a standard calomel electrode (SCE). A graphite block was used as the anode. The current flow in the tank was kept constant by maintaining the submerged area of the graphite block at a fixed ratio with respect to the surface area of the steel parts of the specimen. In an effort to minimize the required size of the graphite block, the loading frame was electrically insulated by coating its surface with paint that was resistant to NaOH.

The specimens were preloaded to an energy release rate of 3.5 kJ/m^2, a level which, based on previous experiments,[5,7] was well within the plateau region. This was checked by using two additional 10° scarf angle specimens which were loaded to energy release rate levels of 4 and 5.4 kJ/m^2. After preloading, the specimens were placed in the NaOH environment and connected to the potentiostat. They were periodically removed in order to measure crack length with vernier calipers. The crack length measurement was made on both sides of the specimens and the average was recorded as the effective crack length. Specimens with deviations in crack lengths that were greater than 1 mm were discarded. The debonding occurred mainly at the primer/steel interface with isolated regions where the locus of failure was between the adhesive and primer. For an energy release rate of 3.5 kJ/m^2, no crack growth was observed in the zero degree scarf specimen ($\phi = 4°$) over a one-

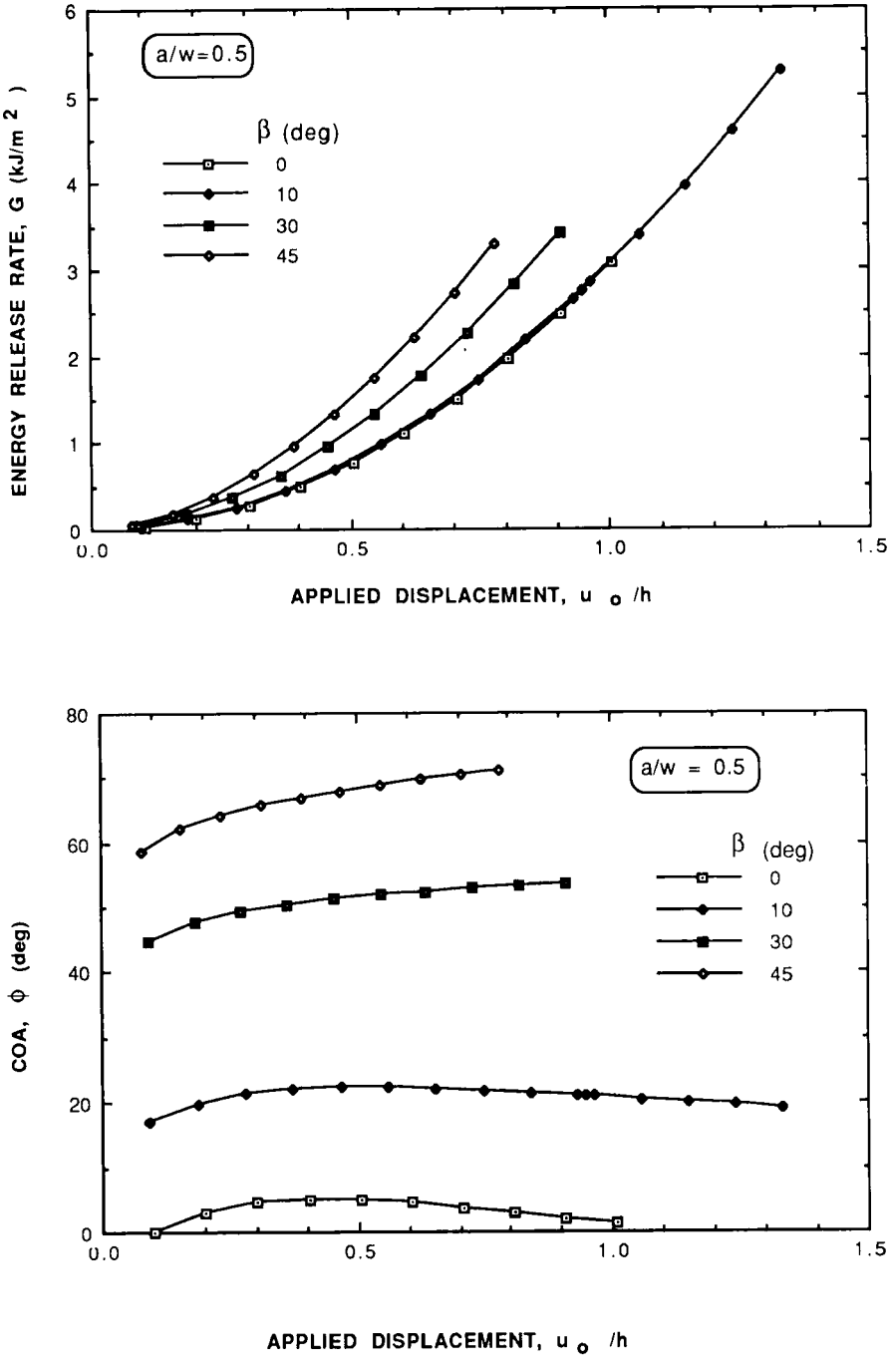

FIGURE 9 Variation of Energy Release Rate and Crack Opening Angle with Load Level and Scarf Angle.

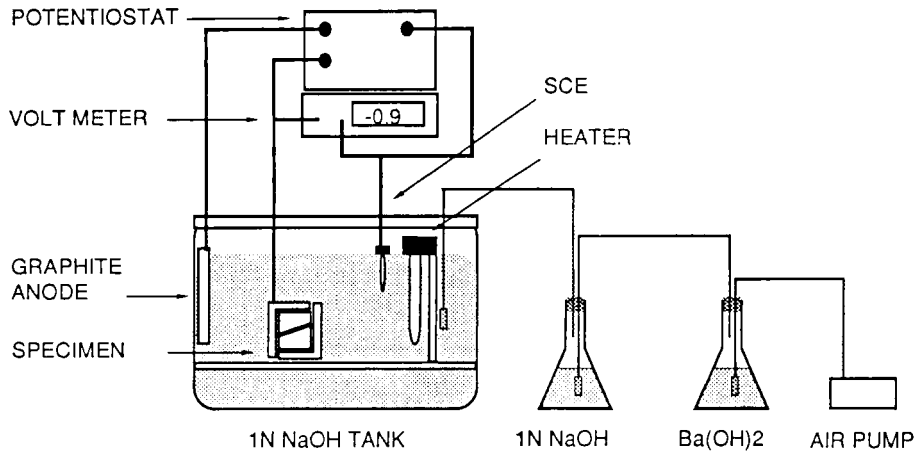

FIGURE 10 Cathodic Delamination Environment.

month period. The histories of cathodic delamination in the other scarf specimens are shown in Figure 11, where it was relatively easy to fit a straight line to the data. The resulting constant delamination growth rates were consistent with the plane-stress analyses which had predicted that energy release rates were independent of crack length. The growth rates increased with increasing scarf angle and are summarized in Figure 12 as a function of energy release rate and crack opening angle. For $\beta = 10°$, there was no variation in crack growth rate with energy release rate (Fig. 12a), thus indicating that energy release rate levels had been properly chosen for the plateau region. Had other energy release rate levels been applied at the other scarf angles, it is therefore reasonable to expect that there would not have been any variation of crack growth rates at a given crack opening angle. The variation in crack growth rate for fixed energy release rate must have been due to the changes in crack opening angle. Increasing the crack opening angle had a dramatic effect on cathodic delamination rates (Fig. 12b). The larger crack opening angles presumably provide for better transport of the chemical species involved in the attack on the bonds closest to the delamination front. Since there is evidence[6] for the formation of a weakly-bonded region ahead of the crack front where attachment is maintained by an array of still-adhering ligaments, increasing crack opening angles would increase the volume of the channels between ligaments and thereby facilitate transport of chemical species.

Limited time and resources did not allow the effect of mode-mix on cathodic delamination outside the plateau region to be examined. However, the results of this investigation give every indication that there could be an effect. Thus, resistance to cathodic delamination will have to be characterized in terms of energy release rates and crack opening angles. In view of the time scale of the experiments, particularly where sea water environments are used, this is a daunting prospect. However, in view of the fact that crack opening angles were nearly independent of load level in the scarf specimens, it may be sufficient to conduct one examination of mode-mix effects for all energy rate levels.

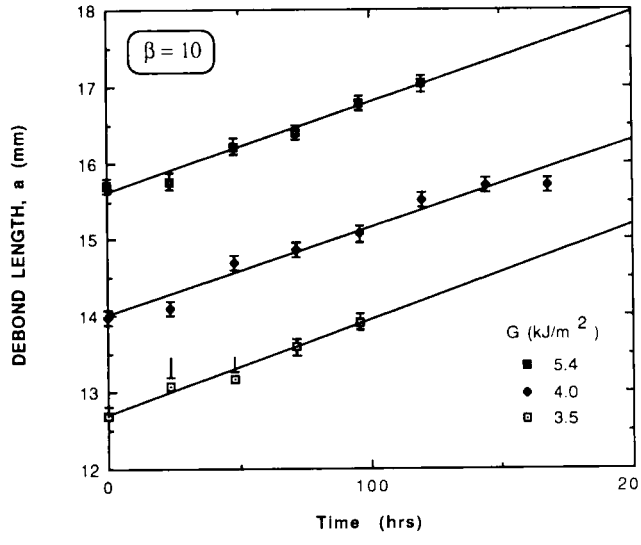

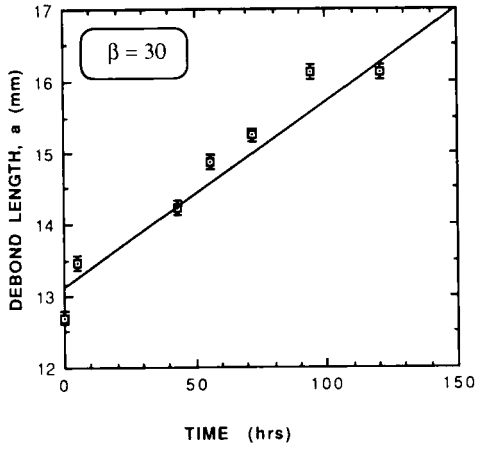

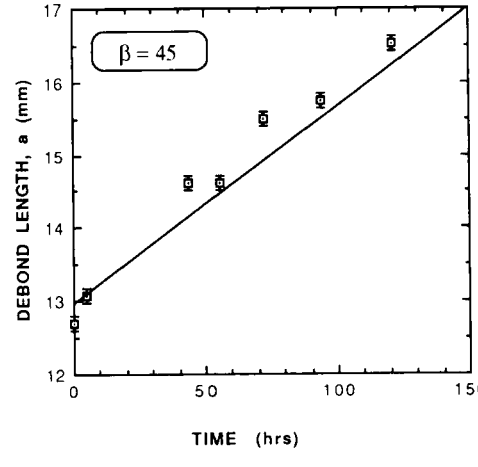

FIGURE 11 Cathodic Delamination Histories.

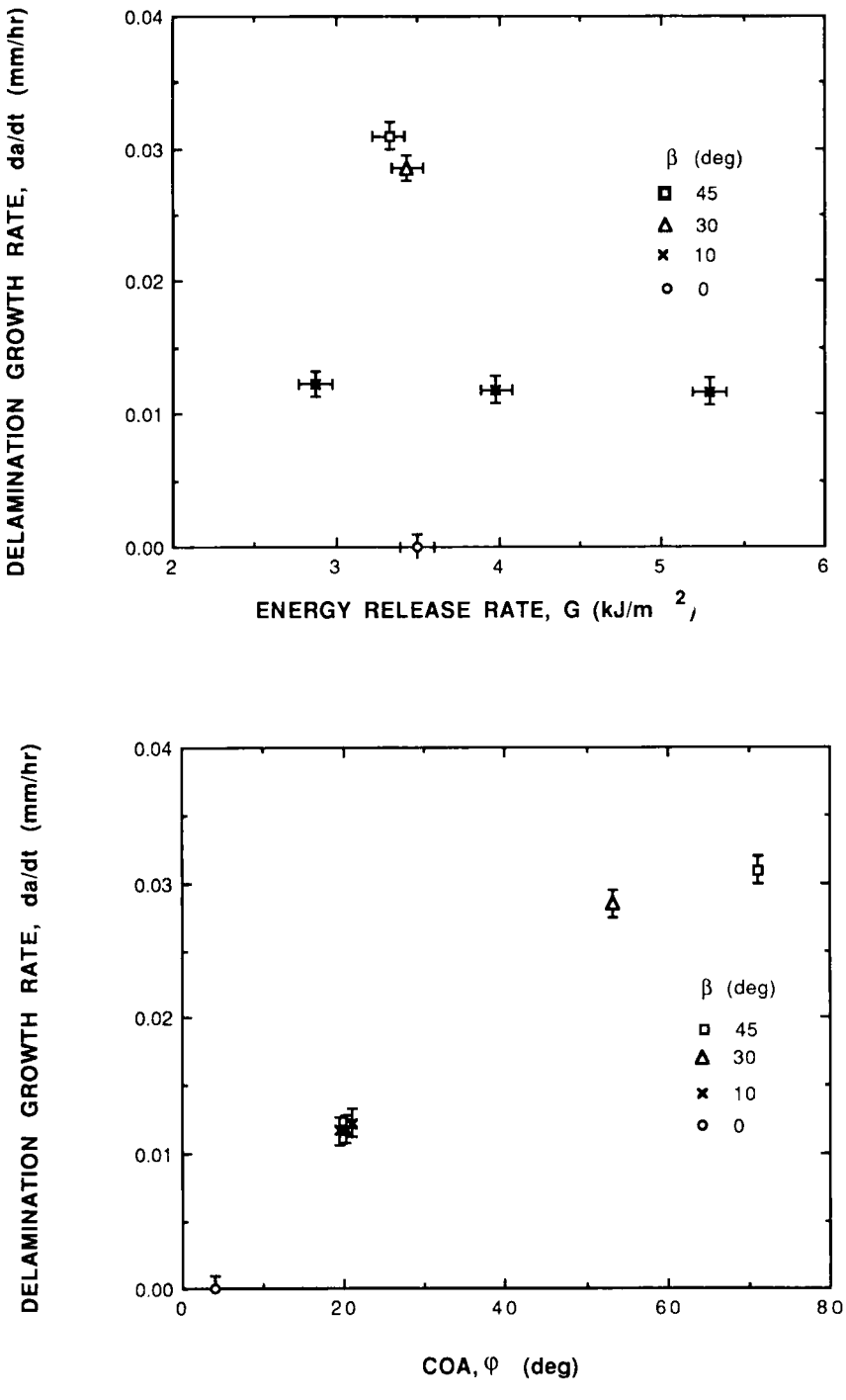

FIGURE 12 Debond Growth Rate Correlations with Energy Release Rate and Crack Opening Angle.

CONCLUSIONS

Single edge-cracked scarf specimens made of a thick Neoprene rubber layer sandwiched between steel adherends were used to examine interfacial cathodic delamination over a range of fracture mode-mixes. The nonlinearly elastic response of the Neoprene 5109S was best represented by the model suggested by Ogden[11] and plane stress analyses were sufficient for the extraction of energy release rates. The crack opening angle appeared to be independent of distance from the crack front for $r<0.5\mu m$ and was used to represent the fracture mode-mix. Specimens with various scarf angles were subjected to a 1N aqueous NaOH environment at 30°C and -0.9 volts with respect to a standard calomel electrode. Cathodic delamination rates were strongly dependent on crack opening angle, probably due to the improved transport of chemical species that is afforded by larger crack opening angles. The cathodic delamination experiments were conducted under displacement control which, in the scarf specimens, produced energy release rates that were independent of crack length. Thus, the cracks were growing into regions where the stresses were neither increasing nor decreasing. In view of the possible interaction with diffusion it is possible that (slowly) accelerating or decelerating cracks would display different characteristics from those encountered under the steady state conditions that prevailed here.

Acknowledgements

The authors would like to acknowledge the support of the Naval Research Laboratory and the Office of Naval Research through subcontracts let from Texas Research International. The respective institutional representatives were Drs. R. W. Timme, L. R. Peebles and J. S. Thornton. The assistance provided by TRI personnel in the specimen preparation phase of the work was invaluable. The authors would also like to thank Drs. Becker and Miller for the use of their computing facilities and the TEXPAC-NL code. Finally, we would like to thank Kriss Hinders and Jan Shrode for their assistance in the preparation of the manuscript.

References

1. A. Stevenson, "The Effect of Electrochemical Potentials on the Durability of Rubber/Metal Bonds in Sea Water," in *Adhesion International* 1987, Proc. 10th Annual meeting of the Adhesion Society, L. H. Sharpe, Ed. (Gordon & Breach, New York, 1987), pp. 137–151.
2. F. J. Boerio, S. J. Hudak, M. A. Miller, and S. G. Hong, "Cathodic Debonding of Neoprene from Steel," *J. Adhesion* **23,** 99–144 (1987).
3. E. L. Koehler, "The Mechanism of Cathodic Disbondment of Protective Organic Coatings-Aqueous Displacement at Elevated pH," *Corrosion-NACE* **40,** 5–8 (1984).
4. H. Leidheiser, W. Wang and L. Igetoft, "The Mechanism for the Cathodic Delamination of Organic Coatings from a Metal Surface," *Progress in Organic Coatings* **11,** 19–40 (1983).
5. K. M. Liechti, E. B. Becker, C. Lin and T. Miller, "A Fracture Analysis of Cathodic Delamination in Rubber to Metal Bonds," *Int. J. Fracture* **39,** 217–234 (1988).
6. R. F. Hamadeh, D. A. Dillard, K. M. Liechti and J. S. Thornton, "A Mechanistic Evaluation of Cathodic Debonding of Elastomer to Metal Bonds," *J. Adhesion Science and Technology* **3,** 421–440 (1989).
7. C. Lin, "Fracture Analysis of Cathodic Delamination in Rubber to Metal Bonds," Engineering Mechanics Research Laboratory Report, EMRL 89/7, Ph.D. Dissertation, December 1989, The University of Texas at Austin.
8. H. M. Jensen, "On the Blister Test for Interface Toughness Measurement," Danish Center for Applied Mechanics **417,** (1990).

9. W. Adamjee, "Mixed-Mode Fracture Analysis of Cathodic Delamination in Rubber Metal Bonds," Engineering Mechanics Research Laboratory Report, EMRL 89/8, MS Thesis, December 1989, The University of Texas at Austin.
10. S. J. Peng, "Nonlinear Multiaxial Finite Deformation Investigation of Solid Propellant, AFRPL-TR-84-036 (1984).
11. R. W. Ogden, "Large Deformation Isotropic Elasticity—On the Correlation of Theory and Experiment for Incompressible Rubberlike Solids," *Proc. Royal Soc. London* **A326,** 565 (1972).
12. E. B. Becker and T. H. Miller, TEXPAC-NL: A Finite Element Code for Elastomeric Analysis, Users Manual (1989).
13. K. C. Valanis and R. F. Landel, "The Strain-Energy Function of a Hyperelastic Material in Terms of Extension Ratios," *J. Appl. Phys.* **38,** 2997–3002 (1967).
14. K. M. Liechti and Y. S. Chai, "Biaxial Loading Experiments for Determining Interfacial Fracture Toughness," *Journal of Applied Mechanics* **58,** 680–687 (1991).
15. D. A. Dillard, K. M. Liechti, D. R. LeFebvre, C. Lin, J. S. Thornton and H. F. Brinson, "The Development of Alternate Techniques for Measuring the Fracture Toughness of Rubber to Metal Bonds in Harsh Environments," **ASTM STP981,** 83–97, (1988).
16. J. K. Knowles and E. Sternberg, "Large Deformations Near the Tip of an Interface Crack Between two Neo Hookean Sheets," *Journal of Elasticity* **13,** 257–293, (1983).
17. G. Ravichandran and W. G. Knauss, "A Finite Elastostatic Analysis of Bimaterial Interface Cracks," *International Journal of Fracture* **39,** 235–253 (1989).